A REINER-RIVLIN FLUID FLOW THROUGH ENTRANCE REGION OF A CIRCULAR PIPE

BY

V.G. Masanja

Department of Mathematics,University of Dar es Salaam
P.O. Box 35062,Dar es Salaam,TANZANIA

ABSTRACT

The flow of a Reiner-Rivlin fluid with two viscosity coefficients through the entrance region of a circular pipe has been studied numerically. In particular the growth of the entrance length as a function of the Reynolds number and the non-Newtonian parameters has been examined. Where comparison could be made, the results have been compared with existing experimental -and numerical data as well as the limited theoretical work available.

INTRODUCTION

The flow of a viscous fluid from a reservoir into a circular tube is encountered in almost every industrial process involving the transport of fluids. As such one of the most widely studied boundary value problems of hydrodynamics is the analysis of the development of the velocity profile of such flows. Information gathered from the study of entrance flows is useful in the analysis of capillary viscometer data on one hand the prediction of viscoelastic entrance behaviour on the other hand.

Various methods have been employed in solving the entrance Region problem. They include the analytical approximate approaches such as the momentum Integral, the kinetic energy End-correction and linearization of inertia terms of the equations of motion. Other approaches are numerical methods based on finite element methods and those based on finite differences. In this analysis, a numerical procedure based on finite differences is employed. Following Greenspan |10| we utilize the stream function vorticity formulation of the problem.

In this work we intend to examine how the velocity profile development and the entrance length vary with the Reynolds number and the non-Newtonian parameter.

The Governing Equations

It is useful to employ Cartesian tensor notation and therefore the summation convention applies to repeated indices and a comma preceding a suffix implies partial differentiation with respect to the corresponding spatial variable. The symbols δji and e_{ijk} denote the familiar Kronecker delta and the alternating tensor, respectively. The continuum theory for viscous fluids requires the velocity vector field $\underline{v}$ to describe the fluid flow with the assumption of incompressibility the mass balance law, $\underline{v}$ is subjected to the constraint

$$v_{i,i} = 0 \tag{1}$$

We restrict ourselves to the steady, laminar flow of a Reiner-Revlin fluid, hence the balance laws for linear momentum reduce to

$$v_{i,j}v_j = \tau_{ij.j} - P_{,j} \tag{2}$$

with thermal effects and external body forces being neglected. Here, ρ is the density assumed constant, τ_{ij} are components of the stress deviator tensor and P is the hydrostatic pressure. The deviatoric stress tensor is given by, |1|,

$$\tau_{ij} = -2\mu_1 d_{ij} + 2/3\mu_2 I_2 \delta_{ij} - 2\mu_2 I_3 d_{ij}^{-i} \tag{3}$$

where μ_1 and μ_2 are viscosity coefficients which are constants, d_{ij} are components of the rate of deformation tensor given by

$$d_{ij} = 1/2 \left[v_{i,j} + v_{j,i} \right], \tag{4}$$

I_2 and I_3 are scalar invariants given by

$$I_2 = d_{ij}d_{ij};\ I3 = \det(d_{ij}) \tag{5}$$

The flow configuration is a circular cylinder hence suitable physical coordinates are cylindrical polar (x,θ,r) for a two-dimensional flow. The equation (1) reduces to

$$v = \frac{v}{u_0},\ u = \frac{u}{u_0},\ r = \frac{r}{a},\ x = \frac{x}{a} \text{ and } p = \frac{P - P_0}{\rho u_0^2} \tag{6}$$

and equations (2) become

$$\rho \left(v\frac{\partial u}{\partial r} + \frac{\partial u}{\partial x} \right) = -\frac{\partial p}{\partial x} - \frac{1}{r}\frac{\partial}{\partial r}\left(r\,\tau_{rx} \right) - \frac{\partial \tau_{xx}}{\partial x} \tag{7}$$

$$\rho \left(v\frac{\partial v}{\partial r} + \frac{\partial v}{\partial x} \right) = -\frac{\partial p}{\partial r} - \frac{1}{r}\frac{\partial}{\partial r}\left(r\,\tau_{rr} \right) - \frac{\partial \tau_{rx}}{\partial x} - \frac{\tau_{\theta\theta}}{r} \tag{8}$$

where τ_{ij} are

$$\tau_{\bar{r}\bar{r}} = -2\mu_1\frac{\partial\bar{v}}{\partial\bar{r}} - 2\mu_2\frac{\bar{v}}{\bar{r}}\frac{\partial\bar{u}}{\partial\bar{x}} + \frac{2}{3}\mu_2 I_2$$

$$\tau_{\bar{r}\bar{x}} = -\mu\left(\frac{\partial\bar{u}}{\partial\bar{r}} + \frac{\partial\bar{v}}{\partial\bar{x}}\right) + \mu_2\frac{\bar{v}}{\bar{r}}\left(\frac{\partial\bar{u}}{\partial\bar{r}} + \frac{\partial\bar{v}}{\partial\bar{c}}\right)$$

$$\tau_{\bar{\theta}\bar{\theta}} = -2\mu_1\frac{\bar{v}}{\bar{r}} - 2\mu_2\frac{\partial\bar{v}}{\partial\bar{r}}\circ\frac{\partial\bar{u}}{\partial\bar{x}} - \frac{2}{3}\mu_2 I_2 \qquad (9)$$

$$\tau_{\bar{x}\bar{x}} = -2\mu_1\frac{\partial\bar{u}}{\partial\bar{x}} - 2\mu_2\circ\frac{\bar{v}}{\bar{r}}\circ\frac{\partial\bar{v}}{\partial\bar{r}} + \frac{2}{3}\mu_2 I_2$$

with
$$I_2 = \frac{1}{2}\left[\left(\frac{\partial\bar{v}}{\partial\bar{r}}\right)^2 + \left(\frac{\partial\bar{u}}{\partial\bar{x}}\right)^2 + \left(\frac{\bar{v}}{\bar{r}}\right)^2\right] - \left(\frac{\partial\bar{u}}{\partial\bar{r}} + \frac{\partial\bar{v}}{\partial\bar{x}}\right)^2 \qquad (10)$$

As customary practice, we introduce the following dimensionless quantities

$$v = \frac{\bar{v}}{u_o},\ u = \frac{\bar{u}}{u_o},\ r = \frac{\bar{r}}{a},\ x = \frac{\bar{x}}{a}\ \text{and}\ p = \frac{p - p_o}{\frac{1}{2}\rho u_o^2} \qquad (11)$$

where a denotes the pipe diameter, uo and po the velocity and pressure at the entrance cross-section respectively. We further introduce the vorticity vector w = curl v whose components are

$$w_i = \varepsilon_{ijk} v_{k,j} \qquad (12)$$

the only non-vanishing component of w being

$$w = \frac{\partial v}{\partial x} - \frac{\partial u}{\partial r} \qquad (13)$$

Utilization of the dimensionless variables from equation (11) and the vorticity from equation (13) transforms equations (7), (8) and (6), respectively, to

$$v\frac{\partial u}{\partial r} + u\left(\frac{\partial u}{\partial x}\right) = -\frac{1}{2}\frac{\partial p}{\partial x} - \frac{1}{rR}\frac{\partial(rw)}{\partial r} + \frac{W}{R}\left[\frac{1}{r}\frac{\partial(vw)}{\partial r} + \frac{\partial}{\partial x}\left[\frac{1}{2}\left(\frac{\partial u}{\partial r} + \frac{\partial v}{\partial x}\right)^2 - \frac{2}{3}I_2\right]\right] \qquad (14)$$

$$v\frac{\partial v}{\partial r} + u\frac{\partial u}{\partial x} = -\frac{1}{2}\frac{\partial p}{\partial x} + \frac{1}{R}\frac{\partial w}{\partial r} - \frac{W}{R}\left[\frac{1}{r}\frac{\partial(vw)}{\partial r} - \frac{\partial}{\partial r}\left[\frac{1}{2}\left(\frac{\partial u}{\partial r} + \frac{\partial v}{\partial x}\right)^2 - \frac{2}{3}I_2\right]\right] \qquad (15)$$

and

$$\frac{1}{r}\frac{\partial(rv)}{\partial r} + \frac{\partial u}{\partial x} = 0 \qquad (16)$$

where

$$Re = \frac{\rho a u_o}{\mu_1} \quad \text{and} \quad W = \frac{\mu_2}{\mu_1} \circ \frac{u_o}{a} \qquad (17)$$

are the Reynolds number and the non-Newtonian parameter respectively.

Taking the curl of equations (14) and (15) eliminates the pressure gradients and reduces (14) and (15) into one equation which, after using (16), is

$$\frac{\partial(uw)}{\partial x} + \frac{\partial(wv)}{\partial r} = \frac{1}{Re}\left[\frac{\partial^2 w}{\partial x} + \frac{\partial}{\partial r}\left(\frac{1}{r}\frac{\partial}{\partial r}\left(r.w\frac{v}{r}\right)\right)\right] \frac{W}{Re}\left[\frac{\partial^2}{\partial x^2}\left(w\frac{v}{r}\right)\right. + \left.\frac{\partial}{\partial r}\left(\frac{1}{r}\frac{\partial}{\partial r}\left(r\circ w\frac{v}{r}\right)\right)\right] \qquad (18)$$

The stokes stream function ψ is introduced through the velocity components

$$u = -\frac{1}{r}\frac{\partial\psi}{\partial r} \quad \text{and} \quad v = \frac{1}{r}\frac{\partial\psi}{\partial x} \qquad (19)$$

such that the mass balance equation (16) is satisfied. With u and v from equation (19) the vorticity equation (13) becomes

$$\frac{\partial^2\psi}{\partial x^2} + \frac{\partial^2\psi}{\partial r^2} - \frac{1}{r}\frac{\partial\psi}{\partial r} - wr = 0 \qquad (20)$$

Replacing u and v in equation (18) by the stream function gradients of equation (19) and some re-arrangement results in the equation

$$\frac{\partial^2\bar{\zeta}w}{\partial x^2} + \frac{\partial^2\bar{\zeta}w}{\partial r^2} + \frac{1\partial\bar{\zeta}w}{r\partial r} - \frac{\bar{\zeta}w}{r^2} R\left[\frac{1}{r}\frac{\partial\psi}{\partial r}\cdot\frac{\partial w}{\partial x} - \frac{1}{r}\frac{\partial\psi}{\partial x}\frac{\partial w}{\partial r} + \frac{w}{r^2}\frac{\partial w}{\partial x}\right] = 0 \qquad (21)$$

where $\bar{\zeta}$ denotes the compression

$$\bar{\zeta} = 1 - \frac{W}{r^2} \circ \frac{\partial\psi}{\partial x} \qquad (22)$$

The simultaneous solution of equations (20) and (21) gives the flow prediction. A numerical procedure based on finite differences is employed. The formulation of the finite difference equations is based on finite Taylor series expansions of relevant variables over

the domain.

Numerical Calculations

The domain of integration is covered with a mesh of rectangular cells of width h and height k. Consider a typical node (0,0) of the mesh (Fig.1) and the surrounding cells. We define the following finite difference operators:

$$\left(\delta_x W\right)_{0,0} = \pm\left(W_{\pm 1,0} - W_{0,0}\right) \; ; \quad \left(\bar{\delta}_x W\right)_{0,0} = \frac{1}{2}\left(W_{1,0} - W_{+1,0}\right)$$

$$\left(\delta_{xx} W\right)_{0,0} = W_{1,0} - 2W_{0,0} + W_{-1,0}$$

$$\left(\delta_r W\right)_{0,0} = \pm\left(W_{\pm 1,0} - W_{0,0}\right) \; ; \quad \left(\bar{\delta}_r W\right)_{0,0} = \frac{1}{2}\left(W_{1,0} - W_{0,-1}\right)$$

and

$$\left(\delta_{rr} W\right)_{0,0} = W_{1,0} - 2W_{0,0} + W_{0,-1} \tag{23}$$

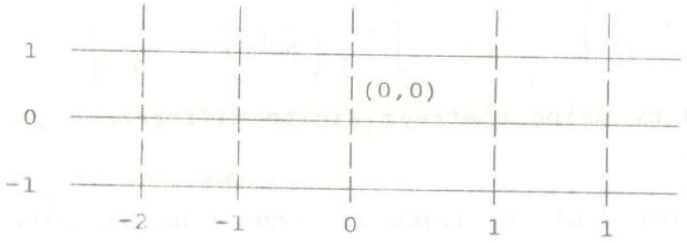

Fig. 1. A typical mesh

With the use of the finite difference operators in equations (23), an approximation for the differential operators appearing in equations (20) and (21) is obtained in the following form

$$\frac{\partial W}{\partial x} = \frac{1}{h}\delta_x W + O(h) = \frac{1}{h}\bar{\delta}_x W + O(h^2); \quad \frac{\partial^2 W}{\partial x^2} = \frac{1}{h^2}\delta_{xx} W + O(h^2)$$

$$\frac{\partial W}{\partial r} = \frac{1}{k}\delta_r W + O(k) = \frac{1}{k}\bar{\delta}_r W + O(k^2); \quad \frac{\partial^2 W}{\partial r^2} = \frac{1}{k^2}\delta_{rr} W + O(k^2) \tag{24}$$

Thus the partial differential equations (20) and (21) are discretized, respectively, as follows:

$$\left(\frac{1}{h^2}\delta_{xx} + \frac{1}{k^2}\delta_{rr} - \frac{1}{rk}\delta_r\right)\psi - wr = 0 \tag{25}$$

$$\zeta\left(\frac{1}{h^2}\delta_{xx} + \frac{1}{k^2}\delta_{rr} + \frac{1}{rk}\delta_r - \frac{1}{r^2}\right)w + R\left(\frac{U}{h}\delta_x + \frac{V}{k}\delta_r - \frac{V}{r}\right)w = 0 \tag{26}$$

with

$$U = -\frac{1}{k}\,\delta_r\psi \;;\; V = \frac{1}{h}\,\delta_x\psi \quad \text{and} \quad \zeta = 1 + \frac{W}{r^2}V \tag{27}$$

If we substitute for the finite difference operators using equations (23), we find that the coefficient of w at the point where equations (26) are applied is:

$$\zeta\left[-2\left(\frac{1}{h^2} + \frac{1}{k^2}\right) \pm \frac{1}{kr_{0,0}} - \frac{1}{r^2_{0,0}}\right] + R\left[\pm\frac{U}{h} \pm \frac{V}{k} - \frac{V}{r_{0,0}}\right] \tag{28}$$

where the + or - signs depend upon the choice of operator in equation (23)

If we consider (26) as a linear system in wi,j, assuming V,V and ζ known, the convergence criterion demands maximization of the diagonal terms of the corresponding matrix of coefficients 2 . By proper selection of signs, it is easy to see that the maximum absolute value of the diagonal term (28) is

$$\zeta\left[2\left(\frac{1}{h^2} + \frac{1}{k^2}\right) + \left|\frac{1}{kr_{0,0}}\right|\right] + R\left[\left|\frac{U}{h}\right| + \left|\frac{V}{k}\right| - \left|\frac{V}{r_{0,0}}\right|\right] \tag{29}$$

which is obtained by using upstream finite differences for first-order derivatives.

The system (25) and (26) of algebraic equations is solved by a successive overrelaxation iterative procedure described in 3 . The correct application of boundary conditions is most important in fluid flow problems and is one of the critical factors affecting convergence particularly in the case of vorticity:

In the entrance region flow through a rigid circular pipe as show in Fig.2 the boundaries are (i) the entrance cross-section (ii) the exit cross-section (iii) the rigid wall and (iv) the axis of symmetry. For solving equation (25) with known values of wi,j we impose that ψ takes a constant value along the wall and along the axis of symmetry; and corresponds to a fully developed flow on the entrance and on the exit cross-sections. For solving equation (26) with known values of ψi,j, again we impose that w, in the entrance and exit sections corresponds to the fully developed flow; on the wall the no-slip condition is assumed so w is calculated from equation (25) with the additional condition that the normal derivative of ψ vanishes while due to continuity w vanishes on the axis of symmetry. Fig.3 shows mesh points, on boundaries, that are used to define finite difference operators for boundary conditions.

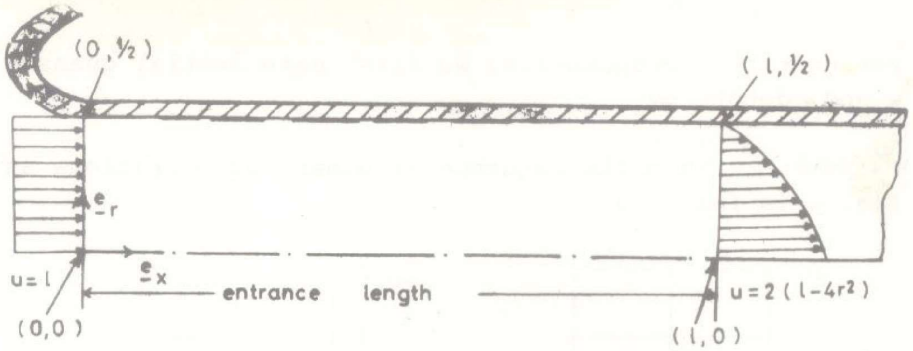

Fig.2: The entrance region flow.

Fig. 2 The Entrance Region Flow

The boundary conditions are, thus, at

the entrance cross-section

$$x = 0,\quad 0 \le r \le \frac{1}{2}\begin{cases} \dfrac{\partial \psi}{\partial x} = 0 \\ \dfrac{\partial \psi}{\partial r} = r \\ \psi = \dfrac{1}{2} r^2 \\ w = 0 \end{cases} \tag{30}$$

the exit cross-section

$$x = 1,\quad 0 \le r \le \frac{1}{2}\begin{cases} \dfrac{\partial \psi}{\partial x} = 0 \\ \dfrac{\partial \psi}{\partial r} = 2r(1-4r^2) \\ \psi = r^2(1-2r^2) \\ w = -16r \end{cases} \tag{31}$$

the axis of symmetry: Assume $\psi = 0$ since $\psi(r=0) = 0$

$$r = 0,\quad 0 \le x \le 1\begin{cases} \dfrac{\partial \psi}{\partial x} = 0 \\ \psi = 0 \\ w = 0 \end{cases} \tag{32}$$

and

the pipe wall: Assume $\psi = 1/a$ since $\psi(r = \frac{1}{2}) = 1/a$

$$r = \frac{1}{2},\quad 0 \le r \le 1\begin{cases} \dfrac{\partial \psi}{\partial x} = 0 \\ \dfrac{\partial \psi}{\partial r} = 0 \\ \psi = -\dfrac{1}{8} \\ w = -2\dfrac{\partial^2 \psi}{\partial r^2} \end{cases} \tag{33}$$

For numerical computations we first make initial guesses for both w and ψ denote by

$w^{(o)}$ and $\psi^{(o)}$ then the sequence of numerical iterations as shown in Fig. 4 is followed.

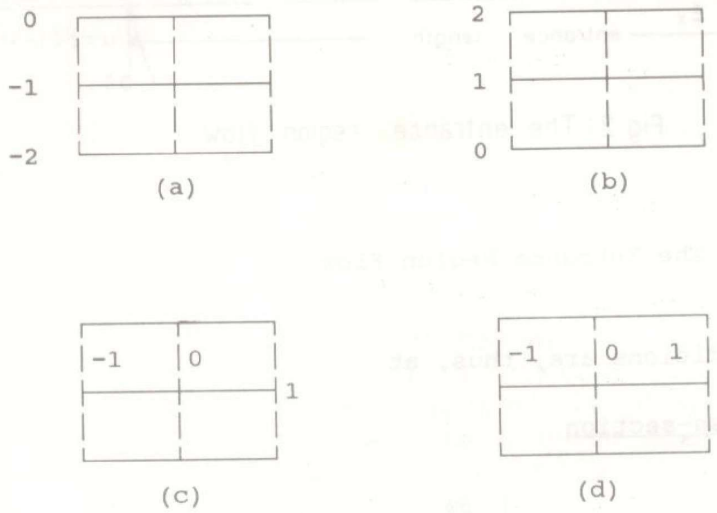

Fig. 3 Boundary cells for (a) the pipe wall, (b) the pipe axis (c) the entrance and (d) the exit-cross section

A complete cycle of iterations is composed of two subcycles for the equations (25) and (26). In each subcycle the field is scanned row by row and a single variable is updated during the scanning process using the appropriate finite difference equations for interior and boundary nodes. A w(1) and w(0) the (1) subcycle is performed and one iteration cycle is thus completed. The procedure is repeated, by substituting new values of w and ψ until the difference between successive approximation is small enough to the desired accuracy or until a prescribed number of iterations is attained.

The velocity components u and v are obtained by numerical differentiation of ψ

$\psi^{(0)}$ $\psi^{(1)}$ $\psi^{(2)}$ $\psi^{(3)}$ $\psi^{(4)}$

$w^{(0)}$ $w^{(1)}$ $w^{(2)}$ $w^{(3)}$ $w^{(4)}$

Fig. 4 The iteration sequence

Numerical Results and Discussion

Numerical results are illustrated graphically in diagrams Fig. 5 to Fig. 10 and tabulated in Table 1 to Table 3. The parameter W give the non-Newtonian character of the fluid. The larger W value is, the more the non-Newtonian influence of the fluid is. R is the Reynolds number based on the pipe diameter and average velocity. R characterizes the inertial influence on the fluid. The larger R gets the more important inertia becomes.

In the foregoing numerical calculations an MxN mesh with maximum size M = N = 31 has been used. The spacing of the mesh lines in the r-directional has been used. The spacing of the mesh lines in the r-directional has been chosen uniform with step size k = so that rj = rj-1 + jk,j = 1(1)N; with r1 = 0. The spacing in the x-directi nal was increased progressively down stream using the formula, |3|

$$xi = \frac{\tan\left(n\left(\frac{i-1}{M-1}\right)\right)}{\tan n}$$

i = 1(1)M; xM = m is the pipe length. The value of m is chosen, for a given r, so as to provide a suitable pipe length whereas the n value is chosen so as to control the density of the grid lines near the entrance of the pipe.

Previous workers such as |4| suggested optimal relaxation parameters for vorticity ξ_ω and stream function ξ_ψ to lie in the range $\xi_\omega \in$ (0.4, 0.8) and (1.0, 1.6). By trial and error the combination (ξ_ω, ξ_ψ) =)0.6, 1.4) was found the best in terms of fastness in convergence.

The convergence criterion was set at ε =10-3 and the number of iterations was limited to 200. Solutions were obtained for the values of R (0, 1000) and W (0.0., 1.0).

One parameter of interest is the inlet length C based on the definition C = xi where xl is the distance along the axis (axial

distance) where the axial velocity reaches 99% of its terminal value, i.e. 1.98. For vanishing non-Newtonian parameter W = 0, the dependence of C on Re has been displayed in Table 1. Comparison of these results with those by previous investigators has been done. The very good agreement of the results confirm the accuracy of the numerical procedure. Table 2 displays the dependence of C on Re and W.

The distribution of axial and radial velocity components u(x,r) and v(x,r), respectively, has been studied over the entire field. Of interest is u(x,r) since the radial velocities are consistently small. Fig. 5 and Fig. 6 show the distribution of u as a function of location for various Re and W values. The centre-line axial velocity, u(x,0) and their dependence on Re and W, respectively, are plotted in Fig. 7 and Fig.8. Finally the effect of Reynolds numbers and non-Newtonnian parameters on the axial velocity profiles are displayed, respectively, by Fig. 9 and Fig. 10.

If we consider W fixed, from Fig. 5, Fig. 7 and Fig. 9 we observe that the fully developed profile is approached faster the higher Re is. For W = 0.0 the results compare favourably with those by other workers such as experimental results by Nikuradse in |5| and numerical results by |6|. Increasing non-Newtonian parameters has the opposite effect to that of Re as it can be seen from Fig. 6, Fig, 8 and Fig. 10. The bigger W is the longer the inlet length is. From Fig. 10 we observe a kink in the velocity profiles that occurs near the entrance cross-section. The kink appears on either side of the axis leading to a pair of symmetrically placed maxima separated by a local minimum of the axis. The kink gets more pronounced the larger W becomes.

Table. 1 Inlet lengths for Newtonian Fluids at high Reynolds Numbers

Investigator	Method Used	Inlet length C
Present Study	Numerical	0.057
Nikuradse in |5|	Experimental	0.063
Schiller in |5|	Momentum Integral	0.029
Campbell & Goldstein in |7|	"	0.061
Atkinson & Goldstein in |5|	Theoretical	0.065
Boussines |5|	"	0.065
Langhaar |8|	Linearization	0.057
Crane & Burley |4|	Numerical	0.056
Baumann & Thiele |6|	"	0.057

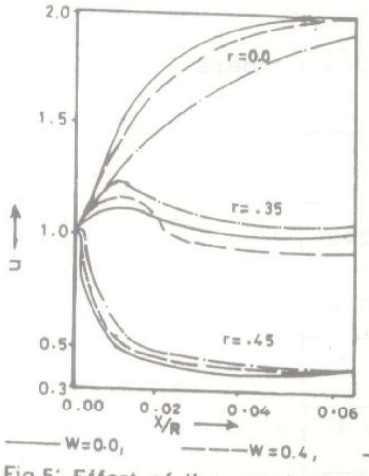

Fig.5: Effect of the non-Newtonian parameter on the axial velocity.

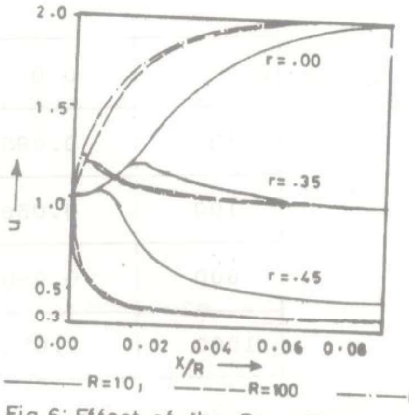

Fig.6: Effect of the Reynolds number on axial velocity.

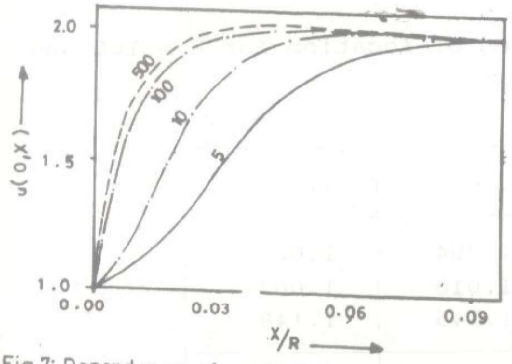

Fig.7: Dependence of centraline axial velocity on the Reynolds number

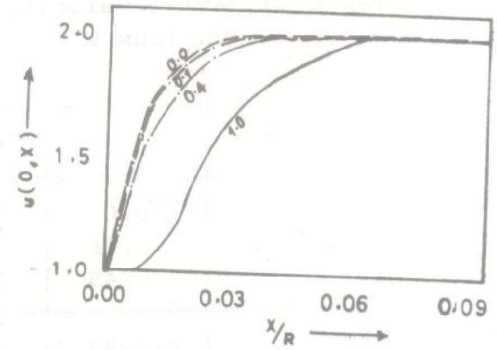

Fig.8: Dependence centraline axial velocity on the non-Newtonian parameter

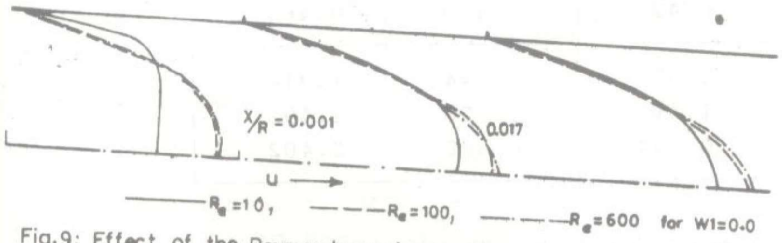

Fig.9: Effect of the Reymonds number on the axial velocity profiles.

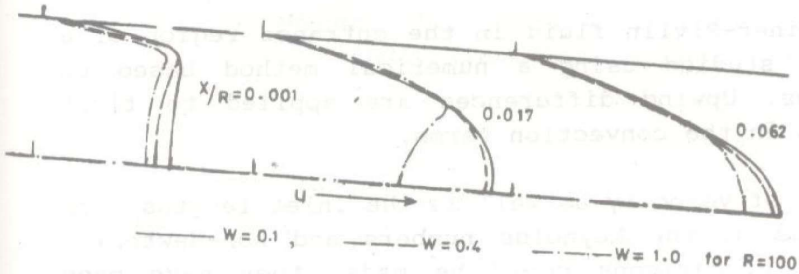

Fig.10: Effect of the non-Newtonian parameter on the axial velocity profiles.

Table 2 Inlet lengths as a function of R and W numbers

R \ W	0.0	0.4	1.0
10	0.0852	0.0969	0.1242
100	0.0568	0.0672	0.1008
600	0.0565	0.0658	
1000	0.0565		

Table. 3 Axial velocity as a function of location for R = 100 and various W

R \ W		0.1	0.4	1.0
0.0006	r=0.00	1.004	1.004	1.003
	0.25	1.012	1.010	1.007
	0.45	1.137	1.145	1.148
0.0247	r=0.00	1.719	1.654	1.477
	0.25	1.487	1.482	1.459
	0.45	0.420	0.430	0.466
0.0485	r=0.00	1.970	1.944	1.814
	0.25	1.497	1.496	1.495
	0.45	0.384	0.388	0.402

Conclusion

The flow of a Reiner-Rivlin fluid in the entrance region of a circular pipe is studied using a numerical method based on finite differences. Upwind differences are applied to first order derivatives in the convection terms.

The distributions of velocity as well as the inlet lengths, are given as functions of the Reynolds numbers and non-Newtonian parameters. Where comparisons could be made they have been made and the good agreement of the results confirm the accuracy of the numerical method.

Acknowledgment

The author wishes to thank the German Academic Exchange Services (DAAD) for financing this study.

Bibliography

|1| Masanja, V.G. (1986) Fortischritt-Berichte VDI Reihe 7:Stromungstechnik Nr. 111, Duseldorf.

|2| Runchal, A.K., (1972), Int. J. Num. Meth. Engng., 4, 541.

|3| Gosman, A.D. et al, (1969), Heat and Mass Transfer in Recirculating flows, Academic Press, London.

|4| Crane, C.M. and D.M. Burley (1976), J. Comp. App. Math., 2,2

|5| Goedstein, S., (1965), Modern Developments in Fluid Dynamics, Vol., 1, Dover Publications Inc. New York, 299 -309

|6| Baumann, W.M. and F. Thiele, (1983), Herman-Fottinger - Institut, IB - 02 (83)

|7| Campbell, W.D. and J.C. Slattery, (1963), Trans. ASME, J. basic Enngg., 85, D. 41

|8| Langhear, H.L. 1942, Jour. App. Mech., 9, A55

|9| Crochet, M.J. and G. Pilate, (1976), J. non-Newtonian Fluid Mech., 1, 247 - 258

|10| Greenspan, D. (1984) Discrete Numerical Methods in Physics and Engineering, Academic Press Inc., New York.